Chemical Engineering Science 61 (2006) 3586–3592

Chemical Engineering Science

www.elsevier.com/locate/ces

Two-dimensional numerical simulations of Marangoni–Bénard instabilities during liquid–liquid mass transfer in a vertical gap

A. Grahn*

Institut für Sicherheitsforschung, Forschungszentrum Rossendorf, P.O. Box 51 01 19, D-01314 Dresden, Germany

Received 23 June 2005; received in revised form 5 January 2006; accepted 7 January 2006

Abstract

Two-dimensional (2D) simulations of isothermal liquid–liquid mass transfer subject to surface tension- and buoyancy-driven hydrodynamic instabilities have been carried out. Simulation is based on the numerical solution of 2D equations of momentum and mass transport, using a combination of finite difference and finite volume methods. Two different cases have been considered: (1) buoyancy stable mass transfer, only surface tension-driven convection occurs; (2) surface tension-driven instability superseeded by buoyant convection. The faster attenuation of mass transfer coefficients in buoyancy stable situations is attributed to the merging of convection cells leading to a reduction in the number of renewal zones along the interface. Concentration profiles next to the interface reveal the diffusional nature of the mass transfer in the immediate interfacial neighbourhood.

Keywords: Convective transport; Diffusion; Mass transfer; Interface; Stability; Simulation

1. Introduction

Mass transfer across interfaces in liquid–liquid systems may give rise to hydrodynamic instabilities and the formation of various dissipative, i.e., convective, structures. Such instabilities are known to considerably enhance mass transfer rates. They are of high interest not only from the fundamental researcher's but also from the engineer's point of view since they make mathematical relations based on diffusional theories inapplicable to chemical reactor design.

Depending on the concentration driving force, fluid properties, the underlying instability mechanism and geometric conditions, such as depth of the liquid layers, shape and extension of the interface, a great variety of convective structures is possible. Lewis and Pratt (1953) observed ripples and erratic pulsations at the surface of solvent drops immersed in water when a solute is transferred between the phases. Orell and Westwater (1962) reported on polygonal cellular convection at the horizontally extended interface during extraction of acetic acid out of ethylene glycol with ethyl acetate. Linde and Schwartz (1989) produced uniaxial roll cells within a narrow vertical gap. Rotational axes of the roll cells aligned with the shorter dimension of the gap geometry. Sherwood and Wei (1957) conducted mass transfer experiments in liquid–liquid systems with a chemical reaction. The mass transfer was accompanied by spontaneous emulsification and the formation of plume-like structures at the interface.

Despite this diversity of phenomena, there are two major mechanisms leading to hydrodynamic instabilities. The first one, referred to as Marangoni effect, is related to the action of surface tension gradients in systems with fluid interfaces while the second one, referred to as Rayleigh–Bénard instability, is related to buoyancy forces. Clearly, both mechanisms may occur simultaneously. Their combined effect on the phenomenology of the mass transfer was investigated by Berg and Morig (1969) using an upright gap geometry, which allowed a quasi-2D flow to develop. The results suggested that density profiles established during the mass transfer may have a strong influence on interfacial convection caused by interfacial tension gradients. In systems with unstable density profiles, buoyant convection penetrated deeply into the bulk phases, superseeding interfacial convection. In stably stratified systems, however, surface tension-driven instability was confined to a

---

* Tel.: +49 351 2602331; fax: +49 351 26012331.
E-mail address: a.grahn@fz-rossendorf.de.

0009-2509/$ - see front matter © 2006 Elsevier Ltd. All rights reserved.
doi:10.1016/j.ces.2006.01.006

narrow zone adjacent to the interface. This ‘confined’ convection organized itself into roll cells, similar to those observed by Linde and Schwartz (1989), which merged to larger cells in the course of the experiment. Measurements of mass transfer rates by Berg and Haselberger (1971) showed extremely high values of the mass transfer coefficient shortly after beginning of the mass transfer, independently of whether buoyant convection was involved or not. At longer contact times, density stable systems yielded mass transfer coefficients closely approximating molecular diffusion values, while density unstable systems persisted on coefficient values being several multiples higher.

By means of holographic interferometry Pertler et al. (1995) detected a steep concentration gradient spreading away from the interfacial zone into the bulk phases. Although the measurement technique was not able to resolve the immediate interfacial neighbourhood, they identified this gradient with the gradient initially present at the interface, postulating a flattening out of the concentration profile there. This interpretation left room for speculations about ‘another transport mechanism’ that must have been in effect at the interface.

In the present study, we report on our investigation of the role that density effects play in the formation of interfacial convection by means of direct numerical simulation. In particular, we were interested in the mechanisms leading to the discrepancy in mass transfer coefficients between density stably and unstably stratified systems. Moreover, clarification about the nature of the mass transport in the immediate vicinity of the liquid–liquid interface was sought. The differential equations, which govern the transport of momentum and chemical species, as well as the numerical solution method are outlined in this paper. A detailed derivation can be found in Grahn (2005, Chapters 5 and 6).

2. Mathematical model

2.1. Governing equations

Convective instabilities driven by solutally induced capillary and buoyant forces are governed by the continuity, the Navier–Stokes and the mass transport equations. For the sake of convenience the model is based on a vertically aligned gap, similar to the flow geometries Berg and Morig (1969), Berg and Haselberger (1971) and Linde and Schwartz (1989) used for their experiments, (Fig. 1). Due to the predominantly two-dimensional and incompressible character of the flow the momentum equations may be cast into the streamfunction-vorticity formulation. Assuming plane Poiseuille flow and using the Boussinesq approximation they may be written

$$\frac{\partial \omega}{\partial t}+\frac{6}{5}\left(u\frac{\partial \omega}{\partial x}+v\frac{\partial \omega}{\partial y}\right)=\nu\left(\frac{\partial^2 \omega}{\partial x^2}+\frac{\partial^2 \omega}{\partial y^2}\right)-\frac{12\nu}{Z^2}\omega-\frac{g_y}{\rho_0}\frac{\partial \rho}{\partial x} \tag{1}$$

and

$$\omega=\frac{\partial^2 \Psi}{\partial x^2}+\frac{\partial^2 \Psi}{\partial y^2} \tag{2}$$

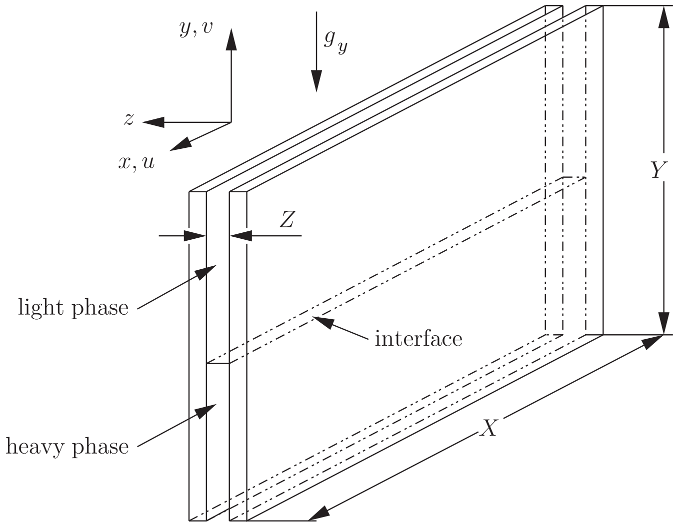

Fig. 1. Schematic view of the gap geometry.

with

$$\omega=\frac{\partial u}{\partial y}-\frac{\partial v}{\partial x}=-(\nabla\times\mathbf{v})_z \tag{3}$$

and

$$u=\frac{\partial \Psi}{\partial y},\quad v=-\frac{\partial \Psi}{\partial x}. \tag{4}$$

Vorticity ω, streamfunction Ψ and velocity components u, v are gap width averaged quantities; ν denotes kinematic viscosity. The second term of the right-hand side of Eq. (1) takes into account the additional drag excerted on the flow by the wall shear stress within a gap of width Z.

If we assume that the solute is advected with gap-averaged velocity and that its concentration does not vary over Z the mass balance equation takes the form

$$\frac{\partial C}{\partial t}+\frac{\partial (uC)}{\partial x}+\frac{\partial (vC)}{\partial y}=D\left(\frac{\partial^2 C}{\partial x^2}+\frac{\partial^2 C}{\partial y^2}\right). \tag{5}$$

The equations of motion and mass transport are coupled by the buoyancy term, velocity and by the interfacial conditions (Section 2.2). Density ρ and interfacial tension σ are correlated to solute concentration C by means of empirical equations

$$\rho=a_0+a_1C+a_2C^2 \tag{6}$$

and

$$\sigma=\frac{1}{1-b_1C}\left[b_2(C-C_{\text{crit}})^2+b_3(C-C_{\text{crit}})^3\right]. \tag{7}$$

Empirical coefficients $a_{0\ldots2}$, $b_{1\ldots3}$ and the critical concentration C_{crit} for the 2-phase/3-component system used in the present study are listed in Appendix A. There are two equations (6) for density, one for each phase, while interfacial tension (7) is related to the interfacial concentration of the lower phase.